ELSEVIER

Journal of Crystal Growth 193 (1998) 712–719

JOURNAL OF CRYSTAL GROWTH

Heat diffusion anisotropy in dendritic growth: phase field simulations and experiments in liquid crystals

R. González-Cinca[a,*], L. Ramírez-Piscina[a], J. Casademunt[b], A. Hernández-Machado[b], T. Tóth-Katona[c], T. Börzsönyi[c], Á. Buka[c]

[a] *Departament de Física Aplicada, Universitat Politècnica de Catalunya, Campus Nord-Ed. B5, J. Girona Salgado s/n, E-08034 Barcelona, Spain*

[b] *Departament ECM, Facultat de Física, Universitat de Barcelona, Diagonal 647, E-08028 Barcelona, Spain*

[c] *Research Institute for Solid State Physics of the Hungarian Academy of Sciences, H-1525 Budapest, P.O. Box 49, Hungary*

Received 27 July 1997; accepted 2 May 1998

Abstract

An anisotropic heat diffusion coefficient is introduced in order to study some interfacial growth phenomena. This anisotropy has been incorporated in a phase field model which has been studied numerically to reproduce some fundamental solidification situations (needle crystal growth) as well as the dynamics of a nematic–smectic-*B* interface. As a general result, we find that dendrites grow faster in the lower heat diffusion direction. Simulation results are compared with experiments with remarkable qualitative agreement.

PACS: 68.70. + w; 61.30. − v; 47.20.Hw

Keywords: Dendrites; Anisotropy; Liquid crystals; Phase field; Interfacial instability

1. Introduction

Dendritic growth has been one of the most studied pattern-forming processes in the last years [1–8]. It takes place in very different contexts such as solidification, electrochemical deposition, phase transitions and viscous fingering in liquid crystals, bacterial growth, etc., and exhibits a very rich behavior. The emergence of the patterns results from the interplay of the stabilizing effect of surface tension and that of interfacial kinetics and the destabilizing effect of a diffusive field (usually temperature or concentration) which controls the motion of the interface. Inherent anisotropies such as that of the surface tension play a fundamental role in the selection of the steady-state shape and its velocity.

The consideration of any kind of anisotropy in the diffusion coefficients, however, has not been taken into account so far, largely because most of

* Corresponding author. Fax: + 34 9 3 4016090; e-mail: ricard@bart.upc.es.

0022-0248/98/$ – see front matter
PII: S0022-0248(98)00505-3

the effort has focussed on the prototypical case of a solid growing from its melt, where the diffusion properties are isotropic. However, systems such as liquid crystals do present considerable anisotropies in their transport coefficients [9–12], and their effects are potentially significant in interfacial growth phenomena.

In this paper we address the growth of dendrites subject to anisotropy in the heat diffusion coefficient, and its consequences on the growth morphologies. In particular, we obtain that the direction of lowest thermal diffusion is preferred, in the sense that the dendrite grows faster in that direction than in the higher-diffusion ones, and that it bends towards the lowest-diffusion direction when set up to grow in any other direction. We present conclusive evidence of these results from both simulation and experiments on liquid-crystal interfacial growth, and provide intuitive arguments to explain this behavior.

2. The model

According to the classical sharp interface model for free solidification, the growth of a pure substance from its melt is controlled by the diffusion of latent heat away from the interface between the phases [7]. This model is completed by the inclusion of two boundary conditions, namely the heat conservation at the interface and the local thermodynamic equilibrium (Gibbs–Thomson relation), corrected by a kinetic term. Usually, anisotropy is included through angular dependences of the surface tension and of the kinetic coefficient, reflecting the dependence of both the average bonding energy between atoms or molecules and the attaching kinetics on the local interface orientation. This anisotropy controls the direction in which dendrites appear. In addition, here we have included anisotropy in the transport properties by means of a heat diffusion tensor. With these elements, the symmetrical (same diffusion coefficient in the two phases) model of solidification is then described by the equations:

$$\frac{\partial T}{\partial t} = \nabla_i D_{ij} \nabla_j T,$$

$$L v_n = n_i D_{ij} c_p [(\nabla_j T)_{\text{solid}} - (\nabla_j T)_{\text{liquid}}],$$

$$T_{\text{interface}} = T_m - \frac{T_m}{L}[\sigma(\theta) + \sigma''(\theta)]\kappa - \beta(\theta) v_n, \tag{2.1}$$

where primes denote derivatives with respect to θ, the angle determined by the orientation of the interface with respect to a crystallographic axis. In these equations D_{ij} are the components of the thermal diffusion tensor, $\sigma(\theta)$ is the anisotropic surface free energy, L is the latent heat per unit volume, v_n is the normal growth velocity of the interface, c_p is the heat capacity per unit volume, T_m is the melting temperature, κ is the local curvature of the interface and n_i are the components of the unit vector normal to the interface. The kinetic coefficient $\beta(\theta)$ describes a departure from local equilibrium associated with dissipation at the moving interface.

In order to perform simulations we employ a phase field model [13–20], which is a usual alternative approach to solve the full time-dependent moving-boundary problem. The phase field model is proven to be a powerful tool to simulate many different physical processes that can be described by the classical sharp interface model. In the phase field approach, both phases and their interface are treated indistinctly, and discriminated by an effective nonconserved order parameter or phase field ϕ, which takes different values in each phase (0 and 1 in our simulations). This field changes smoothly across an interface region of finite thickness, and its dynamics is coupled to that of the temperature field in such a way that the sharp interface model is recovered in the limit of vanishing interface thickness, controlled by a new small parameter ε.

The corresponding dimensionless equations with the three anisotropies included are

$$\begin{aligned}\varepsilon^2 \tau(\theta) \frac{\partial \phi}{\partial t} = {} & \phi(1-\phi)\left(\phi - \frac{1}{2} + 30\varepsilon\alpha\Delta u \phi(1-\phi)\right) \\ & - \varepsilon^2 \frac{\partial}{\partial x}\left[\eta(\theta)\eta'(\theta)\frac{\partial \phi}{\partial y}\right] \\ & + \varepsilon^2 \frac{\partial}{\partial y}\left[\eta(\theta)\eta'(\theta)\frac{\partial \phi}{\partial x}\right] + \varepsilon^2 \nabla[\eta^2(\theta)\nabla\phi],\end{aligned} \tag{2.2}$$

$$\frac{\partial u}{\partial t} + \frac{1}{\Delta}(30\phi^2 - 60\phi^3 + 30\phi^4)\frac{\partial \phi}{\partial t} = \nabla_i K_{ij} \nabla_j u. \tag{2.3}$$

Here temperature is scaled by $T = T_m + \Delta T \cdot u$, where $\Delta T = T_m - T_\infty$ is the undercooling, that is, the difference between T_m and the temperature very far from the moving interface. Lengths are scaled in some arbitrary reference length ω, while times are scaled by ω^2/D_0, where D_0 is the scale of the diffusion coefficient, which is assumed to be the same in both phases. The value of ω is irrelevant for the numerical results. In our simulations we have chosen values of order of the system size. In these equations θ is the angle between the x-axis and the gradient of the phase field.

The dimensionless parameters of the model are

$$\Delta = \frac{c_p \Delta T}{L}, \tag{2.4}$$

$$\alpha = \frac{\sqrt{2}\omega L^2}{12 c_p \sigma(0) T_m} = \frac{\sqrt{2}\omega}{12 d_0}, \tag{2.5}$$

$$\tau(\theta) = \frac{L D_0}{\sigma(0) T_m} \eta(\theta)\beta(\theta), \tag{2.6}$$

$$K_{ij} = \frac{D_{ij}}{D_0}, \tag{2.7}$$

where $\eta(\theta) = \sigma(\theta)/\sigma(0)$, d_0 is the capillary length defined by $d_0 = c_p T_m \sigma(0)/L^2$ (proportional to the surface tension).

We have solved the phase field equations in square lattices using first-order finite differences on a uniform grid with mesh spacing Δx. We have oriented the lattice along the principal directions of the diffusion tensor, so only diagonal terms appear in the simulation associating the principal values of the tensor to the vertical and horizontal directions of the system. On the other hand, in order to clearly distinguish the effects of an anisotropy in the heat diffusion coefficient, we have taken the kinetic term as isotropic (β constant). This means that m is constant in the relation $\tau(\theta) = m\eta(\theta)$.

The equation for the phase field ϕ has been solved by using explicit time-differencing, whereas for the heat equation it has been chosen the alternating-direction implicit (ADI) method, which is unconditionally stable [14]. Both reflecting and constant-temperature boundary conditions have been employed for ϕ and u at the walls of the system. In all cases we have checked the independence of the results on the boundary conditions actually employed provided they are placed far away from the initial nucleus. The growth morphologies are then obtained by setting a seed ($\phi = 0$, $u = 0$) in the lower left corner of the undercooled bath ($\phi = 1$, $u = -1$).

3. Needle crystal growth: simulations and discussion

With the aim of studying the effects of an anisotropic diffusion coefficient on the interfacial growth processes, we have first taken into consideration the evolution of a needle crystal in a solidification process. The surface free energy anisotropy $\sigma = 1 + \lambda \cos(4\theta)$ gives rise to a morphology with four-fold symmetry. When $\sigma + \sigma''$ is positive the equilibrium shape is rounded, and when it is negative, one gets forbidden directions and hence cusps [2]. A value of $\lambda \leqslant 0.0625$ assures us to obtain a rounded shape.

We have started by checking the known results for the selected velocity of the dendrite as a function of the diffusion coefficient in the usual isotropic diffusion case. In Fig. 1a an example of the evolution of two interfaces after the same elapsed time is shown. They are growing from an initial point-like solid seed in a square lattice with 600×600 grid points. The parameters employed in both cases were: $\varepsilon = 0.002$, $\Delta x = 0.005$, $\alpha = 400$, $\Delta = 0.2$, $m = 20$, $\lambda = 0.06$, $\Delta t = 8 \times 10^{-5}$. In the faster growing morphology ($a1$) the diffusion coefficients are $K_{xx} = K_{yy} = 1.2$, while in the slower one ($a2$) we used $K_{xx} = K_{yy} = 0.8$. Hence in these simulations a larger isotropic heat diffusion gives rise to an increase of the interface velocity. This observation is in accordance with analytical results. They predict an increase of the interface velocity with increasing diffusion coefficient in the limit $\mu = p(\Delta)(15\lambda)^{1/2} 2D\beta_0/d_0 < 1$, where $p(\Delta)$ is the Péclet number (see [8]). And simulations performed with different sets of parameters (even corresponding to the opposite limit $\mu \gg 1$, where the choice of parameters leads to decreasing velocity with increasing diffusion coefficient) gave results according to the analytical calculations [8] too.

In Fig. 1b we made a solid seed grow with the same parameters of Fig. 1a but with anisotropic

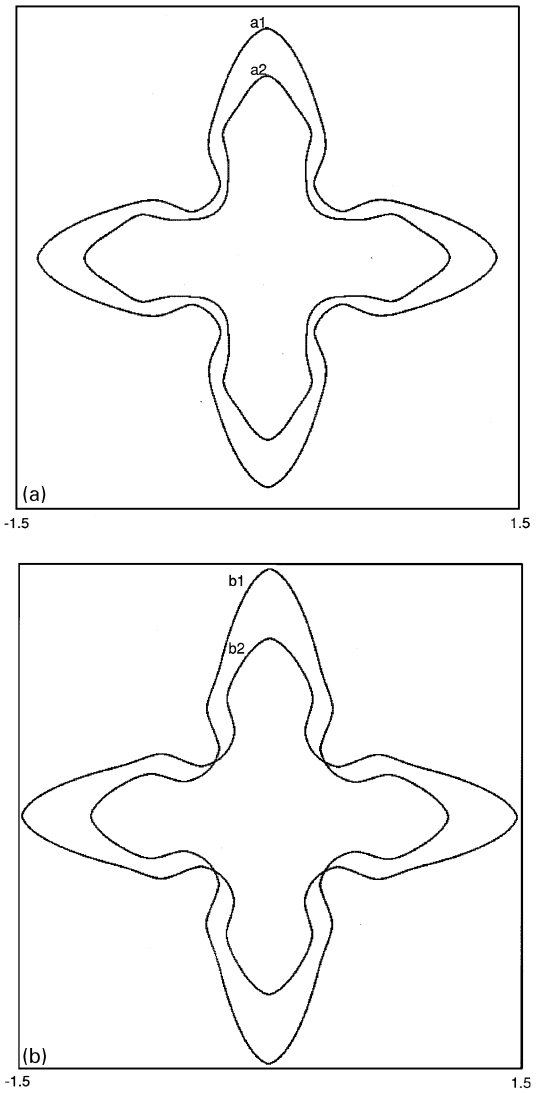

Fig. 1. (a) Growth of two morphologies with isotropic heat diffusion coefficient: 600×600 grid points, $\varepsilon = 0.002$, $\Delta x = 0.005$, $\alpha = 400$, $\Delta = 0.2$, $m = 20$, $\lambda = 0.06$, $\Delta t = 8 \times 10^{-5}$, time = 1.52. ($a1$) $K_{xx} = K_{yy} = 1.2$; ($a2$) $K_{xx} = K_{yy} = 0.8$. (b) Growth of two morphologies with anisotropic heat diffusion coefficient: 600×600 grid points, $\varepsilon = 0.002$, $\Delta x = 0.005$, $\alpha = 400$, $\Delta = 0.2$, $m = 20$, $\lambda = 0.06$, $\Delta t = 8 \times 10^{-5}$, time = 1.52. ($b1$) $K_{xx} = 1.2$ and $K_{yy} = 0.8$; ($b2$) $K_{xx} = 0.8$ and $K_{yy} = 1.2$. The computational domain was reflected around the horizontal and vertical centerlines.

heat diffusion coefficients. The dendrite moving faster in the vertical direction ($b1$) corresponds to values of the diffusion coefficients $K_{xx} = 1.2$ and $K_{yy} = 0.8$. The other dendrite was obtained by exchanging the values of K_{xx} and K_{yy}. It can be seen from the figure that a larger heat diffusion coefficient in one direction gives rise to a lower growth velocity and vice versa. We have obtained the same behavior in all simulations performed for several parameter sets, regardless of what the analytical calculations (see [8]) predict about the velocity dependence on an isotropic diffusion coefficient. Therefore, we conclude that this feature is specific to the anisotropy of the diffusion tensor and that has nothing to do with the kind of dependence of the velocity (increasing or decreasing) on the diffusion coefficient in the isotropic case. Furthermore, faster growth in the low-diffusion direction was also observed in preliminary simulation tests with only anisotropy in the thermal diffusion (neglecting the anisotropy of the surface tension).

In Fig. 2 both dendrites were grown by setting the solid seed in the lower left corner of a square lattice with 400×400 grid points and by rotating the angular dependence of the surface free energy function by $\pi/4$ in the (x, y)-plane. The phase field model parameters used here were: $\varepsilon = 0.002$, $\Delta x = 0.005$, $\alpha = 400$, $\Delta = 0.6$, $m = 20$, $\lambda = 0.0625$,

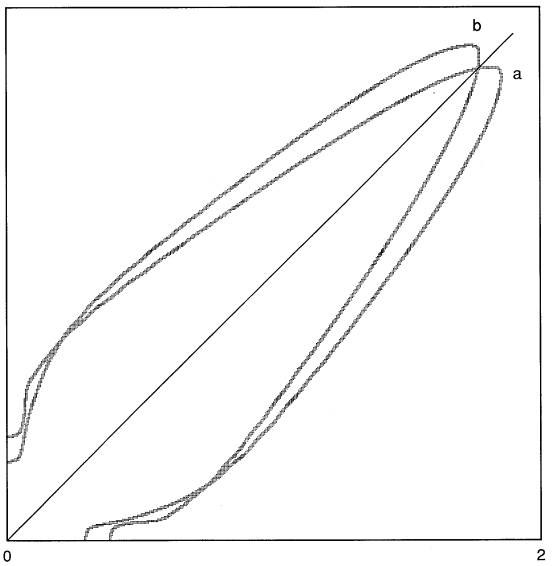

Fig. 2. Tilted parabolas with anisotropic heat diffusion coefficient: 400×400 grid points, $\varepsilon = 0.002$, $\Delta x = 0.005$, $\alpha = 400$, $\Delta = 0.6$, $m = 20$, $\lambda = 0.0625$, $\Delta t = 5 \times 10^{-5}$, time = 0.18. (a) $K_{xx} = 0.8$ and $K_{yy} = 1.2$; (b) $K_{xx} = 1.2$ and $K_{yy} = 0.8$.

$\Delta t = 5 \times 10^{-5}$. In the dendrite (a) the heat diffusion coefficients are $K_{xx} = 0.8$ and $K_{yy} = 1.2$, whereas the exchanged values were used to obtain the other dendrite (b). The dendrite with a larger heat diffusion coefficient in the x direction took a larger angle with this direction and this angle remained constant during the time observed. This angle was exactly $\pi/4$ (i.e. the angle given by the surface tension) in previous simulations with isotropic heat diffusion. Hence, anisotropy in the diffusion tensor is able to change by a certain amount the growing direction of the dendrite, and this change is towards the lower diffusion direction.

In view of these observations one is forced to conclude that for the growth of a dendrite the relevant diffusion process is precisely the one that occurs in the direction transversal to the dendrite propagation. To have a more intuitive picture of that, it may be useful to consider the limiting case in which the diffusion coefficient vanishes in some arbitrary direction. We may ask the question of whether heat can be evacuated at such a growing dendrite at a rate that would permit a constant growth velocity. When the nonzero diffusion direction is that of the dendrite axis, y, the dendrite has to expel heat in the vertical direction. The diffusion in this direction is then one-dimensional, identical to the case of a planar interface, which is known to lack any steady solution for $\Delta \neq 1$. For the interesting case $\Delta < 1$, which is the condition for the existence of the parabolic Ivantsov solution (for most materials accesible undercoolings do verify this condition [2]), the velocity of the planar front goes to zero as $t^{-1/2}$ and therefore the dendrite cannot sustain constant growth. However, in the opposite case with vertical diffusion coefficient equal to zero the dendrite could move expelling heat in the horizontal direction, because all the time the dendrite reaches new cold regions where the released heat has not been able to arrive yet. Moreover, in this case and for a parabolic dendrite growing at constant velocity, any y-fixed point moves horizontally with a velocity that decreases as $t^{-1/2}$, thus compatible with the diffusive behavior of the planar front. In any case it would be interesting to solve the complete selection problem in the general case of nonzero anisotropic diffusion in order to have a more rigorous handling of this behavior.

4. Experiments and simulations of interfacial growth in liquid crystals

An experimental system used to study the thermal diffusion anisotropy is the liquid crystalline substance CCH_4 (4-n-butyl-4′-cyano-trans-1,1-bicylohexane). We have focused on the first order nematic–smectic-B phase transition for large undercoolings (see a more detailed study of this substance in [19]). The experimental system consisted of a thin sample ($d = 10$ μm) with the nematic director oriented parallel to the bounding glass plates ((x, y)-plane of the observation) along the y-direction. The quasi two-dimensional geometry of the samples has been achieved by adequate choice of their linear dimensions (1.5 cm × 1.5 cm in the (x, y)-plane).

When the sample is undercooled below the transition temperature T_m some smectic-B nuclei appear and grow, giving rise to different growing shapes of the interface depending on the value of the undercooling ΔT.

Although the average thermal diffusion coefficient D and its anisotropy $D_a = (D_{yy} - D_{xx})/D_{xx}$ (where D_{yy} and D_{xx} are the coefficients parallel and perpendicular to the director, respectively) have not been measured, some estimation can be obtained by comparison with other liquid crystals. The values of D and D_a do not differ significantly in the two phases considered [9,10] and D_a is positive [11]. Moreover, we can assume that D_a is approximately 0.5 (for a more detailed discussion see [19]).

The angular dependence of the surface free energy has been obtained by measuring the equilibrium shape of the nematic–smectic-B interface, and by using the Wulff construction. This is a geometrical method based on the idea that in thermal equilibrium the surface free energy is minimized. The expression for the angle dependence of the surface free energy is then $\eta(\theta) = 1.000 - 0.445\theta^2 + 0.026\theta^4$ ($0 \leqslant \theta \leqslant \pi/2$), where $\theta = 0$ corresponds to the direction perpendicular to the smectic director.

In the large undercooling regime ($\Delta T \geqslant 0.3^\circ$C) a shape of the growing smectic-B phase with four main dendrites has been observed (see Fig. 3). The (smaller) angle α between main branches varies from 0° to 60° depending on the nucleation point. The director of the smectic-B phase was found to lie

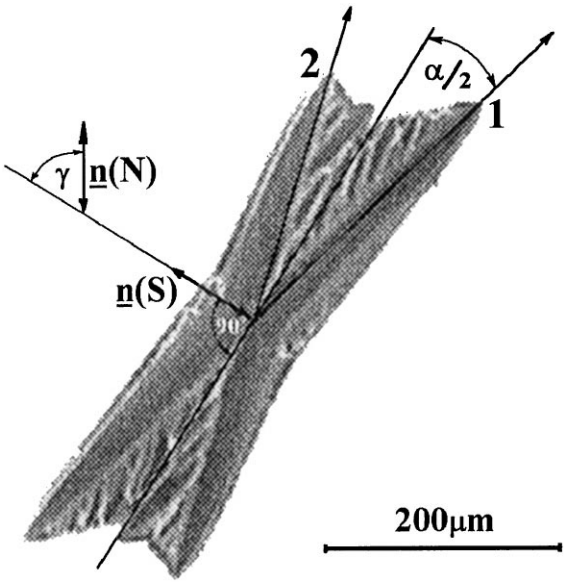

Fig. 3. Snapshot of the growing smectic-B phase of CCH_4 showing the nonreflection symmetry of the dendrites. $\boldsymbol{n}(N)$ and $\boldsymbol{n}(S)$ – director of the nematic and smectic-B phases, respectively; α – the (smaller) angle between the main branches; γ – angle between $\boldsymbol{n}(N)$ and $\boldsymbol{n}(S)$; 1 and 2 denote main branches with growth velocities v_1 and v_2, respectively.

in the (x, y)-plane. It has been also observed that the angle γ between the orientation of the smectic-B object, fixed by the smectic director $\boldsymbol{n}(S)$, and the director of the surrounding nematic $\boldsymbol{n}(N)$ varies from 0° to 80°. In all experiments, the smectic director has been found perpendicular to the bisectrix of the angle α. When $\gamma \neq 0$ and $\gamma \neq 90^\circ$, a nonreflection symmetry appeared in the growth shape (except the case of $\alpha = 0$). This means that the pair of main branches with opposite growth direction, which have a larger angle with the nematic director, have larger growth velocity (with an absolute value of v_1) than the other pair (v_2) (see Fig. 3). The observed relative difference in the growth velocities $\delta v = (v_1 - v_2)/v_1$ in some cases reached the value of 0.2. An asymmetry has also been observed in the side-branching activity with respect to the growth direction of the main dendritic tip, which was studied in [19].

Taking into consideration the uniaxial nature of the nematic phase, a nonmonotonous angular dependence $\delta v(\gamma)$ with a maximum in the middle of the range $0^\circ < \gamma < 90^\circ$ can be expected. Experimental results confirmed such a relation (see Fig. 4). In Fig. 4, for quantitative comparison only the smectic objects with α in a narrow range ($27^\circ \leqslant \alpha \leqslant 34^\circ$) are considered in order to have at least approximately similar interplay between the main branches. Unfortunately, direct analysis of the tip growth velocity (v) dependence on the growth direction was not possible, since a strong dependence of v on the type of the nucleation point (impurities, orientational defects of the director or defects on the bounding glass plates) has been observed and reported in [19].

Note that $\eta(\theta)$ will also be modified by anisotropic elastic contribution in the case of $\gamma \neq 0$ which should decrease the anisotropy of the surface tension (see more detailed discussion in [21]), but this contribution could not be detected.

The growth of interfaces in liquid crystals is mainly controlled by the diffusion of latent heat away from the interface as in solidification processes. Interfacial growth in liquid crystals can then be also described by a symmetrical sharp interface model, differing from solidification in the magnitude of some parameters. Thus, we are allowed to simulate the growth of the nematic–smectic-B interface in CCH_4 by means of the phase field model (Eqs. (2.2), (2.3), (2.4), (2.5), (2.6) and (2.7), where now the smectic-B and the nematic play the role of the solid and liquid, respectively). Some of the results obtained from these simulations have already been presented in [18,19], where with the sole introduction of anisotropy in the surface free energy, the quasi-equilibrium and spontaneous nucleation morphologies for the case of $\gamma = 0$ were qualitatively reproduced. Here, we show that by rotating the surface free energy function in the (x, y)-plane, and by adding an anisotropic heat diffusion coefficient we can also reproduce the experimentally observed morphologies of the interface with $\gamma \neq 0$ which show the nonreflection symmetry.

In the numerical simulation of this case, we have used a lattice of 600×600 grid points, setting the initial smectic-B seed in the center of the square. The parameters employed are: $\varepsilon = 0.005$, $\Delta x = 0.005$, $\alpha = 850$, $\Delta = 0.5$, $m = 20$, $\Delta t = 2 \times 10^{-6}$. Although this set of parameters could differ from

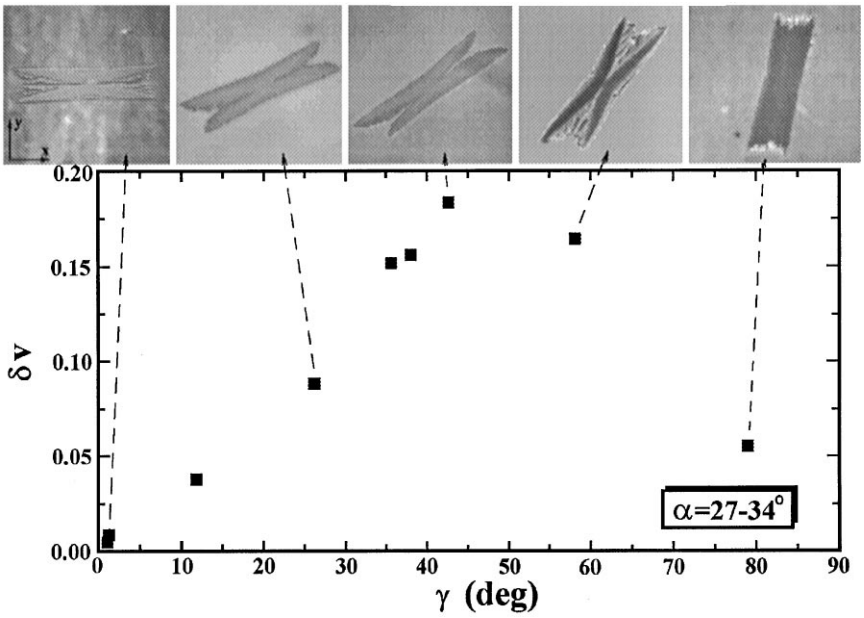

Fig. 4. Experimental results showing the relative difference in the growth velocities $\delta v = (v_1 - v_2)/v_1$ of the main branches versus the angle γ ($\Delta T = 1.00^{\circ}$C). In the upper part of the figure smectic objects with different γ are shown (the nematic director is parallel with y in each case).

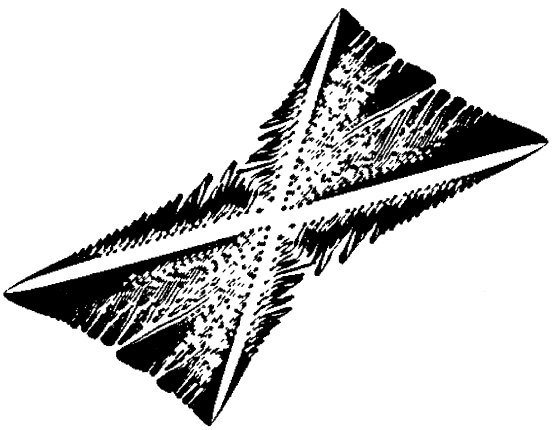

Fig. 5. Simulation for the nonreflection symmetry: 600×600 grid points, $\varepsilon = 0.005$, $\Delta x = 0.005$, $\alpha = 850$, $\Delta = 0.5$, $m = 20$, $\Delta t = 2 \times 10^{-6}$, time $= 0.06$. $K_{xx} = 0.4$, $K_{yy} = 0.6$, $D_a = 0.5$.

those real material ones, the qualitative resemblance is remarkably good. The heat diffusion coefficients used were $K_{xx} = 0.4$ and $K_{yy} = 0.6$ and its anisotropy was $D_a = 0.5$, being very similar to what was expected experimentally, as it has been stated before. In Fig. 5 the morphology obtained in the described simulation is shown. As can be seen, the reflection symmetry has been broken by including the anisotropic heat diffusion only (previous simulations with rotated surface tension function and isotropic heat diffusion did not show the asymmetry in the growth velocities). In both experiments and simulations the most developed branches are systematically those growing in the direction of lowest heat diffusion, consistent with the general results of the previous section.

5. Conclusions

In summary, we have presented some numerical results of the role that an anisotropic heat diffusion coefficient plays in dendritic growth. We have concluded that heat diffusion anisotropy favors dendritic growth in the lowest diffusion directions. This means that the relevant heat diffusion process is the one that occurs in the direction perpendicular to the axis of the dendrite. Although this result may seem counterintuitive, we have provided simple

arguments based on extreme situations which support this scenario. Finally, we have shown that these results can explain some experimental observations made for lower symmetry phases growing with different orientation into a higher-symmetry nematic with strong anisotropies in its transport coefficients.

Acknowledgements

Authors wish to thank Prof. L. Kramer for many fruitful discussions. Á.B. is indebted to the hospitality of the University of Barcelona and Politechnical University of Catalunya. R.G.C. is indebted to the KFKI for its kind hospitality and assistance. Investigated substances were kindly made avaliable for us by Merck, Darmstadt. The work was financially supported by EU TMR Project No. ERB FMRX-CT 96-0085 and by the Hungarian Academy of Sciences Grants No. OTKA T014957 and OTKA F022771. R.G.C., L.R.P., J.C. and A.H.M. thank the Dirección General de Investigación Científica y Técnica (Spain) (Projects PB96-0241-C02-02, PB96-1001-C02-02, PB96-0378-C02-01) for support. We also acknowledge the Centre de Supercomputació de Catalunya (CESCA) for computing support.

References

[1] P. Pelcé (Ed.), Dynamics of curved fronts, Perspectives in Physics, Academic Press, New York, 1988.
[2] C. Godrèche (Ed.), Solid far from Equilibrium, Cambridge University Press, Cambridge, 1992.
[3] D.T.J. Hurle (Ed.), Handbook of Crystal Growth, vol. 1B, North-Holland, Amsterdam, 1993.
[4] P.E. Cladis, P. Palffy-Muhoray (Eds.), Spatio Temporal Patterns, Santa Fe Institute Studies in the Science of Complexity, vol. XXI, Addison-Wesley, Reading, MA, 1994.
[5] P.P. Trigueros, J. Claret, F. Mas, F. Sagués, J. Electroanal. Chem. 312 (1991) 219.
[6] E. Ben-Jacob, P. Garik, Nature 343 (1990) 523.
[7] J.S. Langer, in: J. Souletie, J. Vannimenus, R. Storra (Eds.), Lectures in the Theory of Pattern Formation, Chapter 10 in Chance and Matter (1986 Les Houches Lectures), North Holland, Amsterdam, 1987, pp. 629–711.
[8] E.A. Brener, V.I. Melnikov, Adv. Phys. 40 (1991) 53.
[9] F. Rondelez, W. Urbach, H. Hervet, Phys. Rev. Lett. 41 (1978) 1058.
[10] U. Zammit, M. Marinelli, R. Pizzoferrato, F. Scudieri, S. Martellucci, Phys. Rev. A 41 (1990) 1153.
[11] H. Hervet, F. Rondelez, W. Urbach, Transport properties in liquid crystals, in: S. Chandrasekhar (Ed.), Liquid Crystals, Heyden, London, 1980, p. 263.
[12] G.J. Krüger, Phys. Rep. 82 (1982) 231.
[13] R. Kobayashi, Physica D 63 (1993) 410.
[14] A.A. Wheeler, B.T. Murray, R.J. Schaefer, Physica D 66 (1993) 243.
[15] G.B. McFadden, A.A. Wheeler, R.J. Braun, S.R. Coriell, R.F. Sekerka, Phys. Rev. E 48 (1993) 2016.
[16] S.-L. Wang, R.F. Sekerka, A.A. Wheeler, B.T. Murray, S.R. Coriell, R.J. Braun, G.B. McFadden, Physica D 69 (1993) 189.
[17] R.J. Braun, G.B. McFadden, S.R. Coriell, Phys. Rev. E 49 (1994) 4336.
[18] R. González-Cinca, L. Ramírez-Piscina, J. Casademunt, A. Hernández-Machado, L. Kramer, T. Tóth Katona, T. Börzsönyi, Á. Buka, Physica D 99 (1996) 359.
[19] T. Tóth-Katona, T. Börzsönyi, Z. Váradi, J. Szabon, Á. Buka, R. González-Cinca, L. Ramírez-Piscina, J. Casademunt, A. Hernández-Machado, Phys. Rev. E 54 (1996) 1574.
[20] A. Karma, W.J. Rappel, Phys. Rev. E 53 (1996) 3017.
[21] Á. Buka, T. Tóth-Katona, L. Kramer, Phys. Rev. E 49 (1994) 5271.